Applied Physics Express **5** (2012) 011101
DOI: 10.1143/APEX.5.011101

Ionoluminescence as Sensor of Structural Disorder in Crystalline SiO_2: Determination of Amorphization Threshold by Swift Heavy Ions

Ovidio Peña-Rodríguez[1,2*,†], David Jiménez-Rey[1*], Javier Manzano-Santamaría[1,3], José Olivares[1,2], Angel Muñoz[1], Antonio Rivera[4], and Fernando Agulló-López[1]

[1]*Centro de Microanálisis de Materiales (CMAM), Universidad Autónoma de Madrid (UAM), Cantoblanco, E-28049 Madrid, Spain*
[2]*Instituto de Óptica, Consejo Superior de Investigaciones Científicas, C/ Serrano 121, E-28006 Madrid, Spain*
[3]*Euratom/CIEMAT Fusion Association, Madrid, Spain*
[4]*I. de Fusión Nuclear, Universidad Politécnica de Madrid, C/ José Gutiérrez Abascal 2, E-28006 Madrid, Spain*

Received September 26, 2011; accepted November 19, 2011; published online December 15, 2011

Ionoluminescence (IL) has been used in this work as a sensitive tool to probe the microscopic electronic processes and structural changes produced on quartz by the irradiation with swift heavy ions. The IL yields have been measured as a function of irradiation fluence and electronic stopping power. The results are consistent with the assignment of the 2.7 eV (460 nm) band to the recombination of self-trapped excitons at the damaged regions in the irradiated material. Moreover, it was possible to determine the threshold for amorphization by a single ion impact, as ~1.7 keV/nm, which agrees well with the results of previous studies.

Silicon dioxide (SiO_2), either crystalline (quartz) or amorphous (silica), is a relevant compound very abundant in nature that presents many applications in a large variety of fields ranging from photonics and microelectronics to geology (dating) and archaeology. In several of these technologies both materials are subjected to high fluxes of radiation, such as photons in laser technology, or neutrons and charged particles in accelerators and nuclear fission and fusion installations.[1,2] However, most previous works concerned with the effects of irradiation on these materials have been focused on the effect of UV light, X-rays, electrons, neutrons and ions on amorphous silica[3–7] but less attention has been paid to the irradiation effects on the crystalline phase (quartz).[8–10] Interest in the damage produced by heavy-mass high-energy (i.e., swift heavy) ions has strongly increased recently because electronic mechanisms are dominant over elastic nuclear collisions and the induced damage presents a number of differential features not yet sufficiently understood.[11–15] On the other hand, luminescence[16,17] is a very sensitive technique often applied for the characterization of dielectric and semiconductor materials. In particular, for ion-beam irradiation, the induced luminescence, ionoluminescence (IL), is an appropriate technique for investigating the microscopic processes accompanying the generation of damage and the formation of color centers.[5,6,18,19] Unfortunately, the analysis of the data obtained by this technique is not simple and generally requires additional data, from other optical techniques such as optical absorption and photoluminescence (PL), in order to obtain physically meaningful information.

This work focuses on the ionoluminescence induced on α-quartz by irradiation with swift heavy ions. In this case, very little IL information is available except for some data obtained on synthetic[19] and natural[20] quartz using light ions. However, it is now well known[12,13] that every swift ion impact generates a well-defined amorphous track of nanometer diameter whenever the electronic stopping power is above a certain threshold value. Moreover, the damage is cumulative so that, even below the threshold, amorphization can still be achieved through track overlapping. The IL spectra and yields will be discussed within such a scheme, so that new relevant information might be obtained on track formation and crystal amorphization. In particular, it will be shown that IL allows for a reliable determination of the amorphization threshold.

Table I. Irradiation parameters, where S_e is the stopping power at the surface and R_p is the projected ion range.

Ion	Energy (MeV)	S_e (keV/nm)	R_p (μm)
B^{2+}	3	1.1	3.8
O^{2+}	4	1.9	3.5
F^{2+}	5	2.2	3.7
Cl^{2+}	5	2.9	3.0
Cl^{3+}	10	3.8	4.4
Br^{4+}	15	4.7	5.5
Br^{5+}	25	6.1	7.3

The quartz samples used in this paper were prepared from 1-mm-thick crystal wafers (z-cut) provided by Crystran. They were cut into pieces of about $10 \times 10\,mm^2$ and covered by a copper mask to define an irradiation area of $6 \times 6\,mm^2$ (slightly smaller than the ion beam size) and also to avoid electrical discharges. Samples were irradiated in a standard scattering chamber, at a vacuum of 10^{-4} Pa, connected to a 5 MV tandem accelerator in the Centro de Microanálisis de Materiales (CMAM).[21] They were tilted 5° to avoid the ion channeling condition. The beam homogeneity, essential for this work, was carefully checked to be within 10% by means of the ionoluminescence induced in a sample of amorphous SiO_2 monitored with a 12-bit charge-coupled device (CCD) camera. Irradiation was performed with the ions and energies listed in Table I, using currents in the range 10–30 nA to avoid overheating of the samples. The IL emission was transmitted through a silica window port placed at 45° to the ion beam and collected and focused with a 25-mm-diameter, 4-cm-focal-length silica lens into a silica optical fiber of 1 mm diameter. The light was guided to a compact spectrometer, QE6500 (Ocean Optics), configured with a multichannel array detector for measuring simultaneously the whole spectrum in the range 200–850 nm with a spectral resolution better than 2 nm. The light integration time was varied between 1 and 5 s.

Figure 1 shows the IL emission spectra induced on alpha quartz by Br at 25 MeV at the beginning [Fig. 1(a)] and at the

*These two authors contributed equally to this work.
†E-mail address: ovidio.pena@uam.es

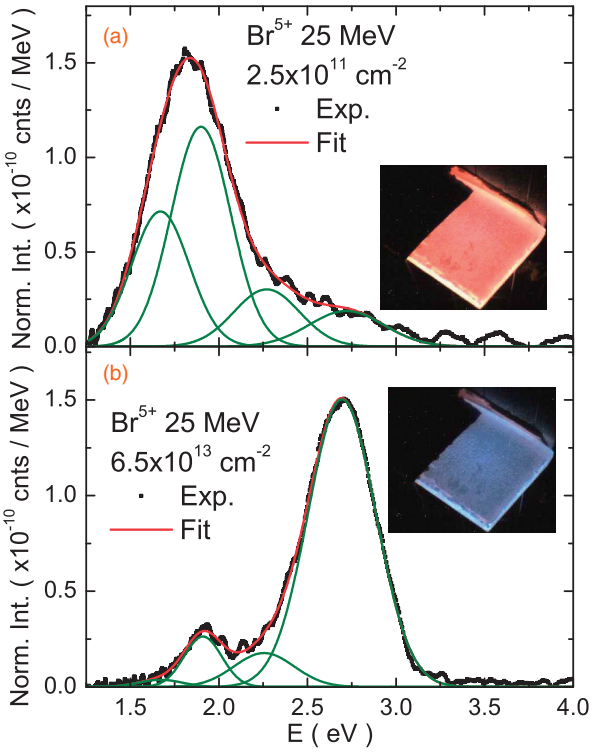

Fig. 1. IL spectra, and analysis of their component bands, during irradiation of quartz with Br at 25 MeV. (a) Low irradiation fluence (2.5×10^{11} cm^{-2}) and (b) high irradiation fluence (6.5×10^{13} cm^{-2}). The insets represent color photos of the samples showing the transition from red to blue with progressing irradiation.

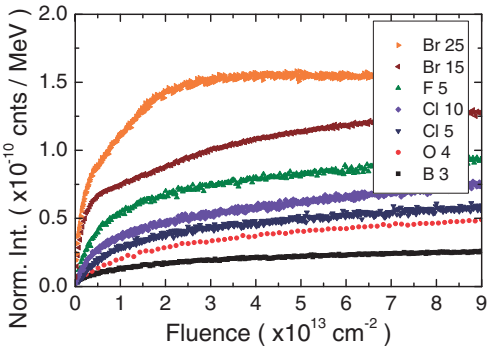

Fig. 2. Overall kinetics for the normalized yield of the blue (2.7 eV) band (see text) as a function of the irradiation fluence. The curves correspond, from bottom to top, to the ions B (3 MeV), O (4 MeV), Cl (5 and 10 MeV), F (5 MeV), and Br (15 and 25 MeV).

end [Fig. 1(b)] of the irradiation. The inset photos illustrate the change in color from reddish to blue on increasing the levels of damage. Note that this case corresponds to irradiation conditions above the expected electronic stopping power threshold for amorphization (≈2 keV/nm) at the sample surface.[22–24] Two broad emission bands can be seen at 1.9 eV (670 nm) and 2.7 eV (460 nm). Two weaker bands can also be observed at 1.65 and 2.26 eV. The red emission at 1.9 eV is initially dominant but it is gradually converted into blue emission as the irradiation progresses. The blue emission at 2.7 eV becomes overwhelmingly dominant above 10^{13} cm^{-2}. All those observations are consistent with the assignment of the red band to color (NBOHC) centers,[5,8,25] whereas the blue band is associated with the radiative emission of a self-trapped exciton in the intrinsic but distorted SiO_2 network.[26] This assignment has been inferred from the results of detailed spectroscopic studies[10] and supported by theoretical considerations[27,28] that predict efficient self-trapping of excitons in silica, where Si–O bonds are strongly distorted, but not in crystalline quartz.

The blue band carries the main structural information, particularly on the initial linear region of the curves, before more complex processes take effect and modify the structure of damage. Its kinetics as a function of fluence is given in Fig. 2 for the whole manifold of ions and energies used in this work. It consists of an initial fast linear stage followed by a saturating or low-growth stage. Pending a more complete discussion we will adopt here a phenomenological scheme based on the analysis of the time and space scales involved in the irradiation process. In a sub-femtosecond scale, a dense and hot electron–hole cloud (i.e., the incoherent bunch of electrons and holes produced by every ion impact) is generated and reaches thermal equilibrium[12] through electron–electron interaction in about 10^{-14} s. The initial energy distribution[29] around the ion trajectory, with a width of around one nanometer, acts as an initial condition for the process. Then, the electron–phonon interaction sets in and a thermal electron–lattice equilibrium is reached in $\sim 10^{-13}$–10^{-12} s. The linear lattice region around the ion trajectory reaches a high temperature (*thermal spike*) and a high electron–hole density (*excitation spike*) and has a diameter of several nanometers. Then, the system cools down rapidly and *point defects*, as well as an *amorphous track*, may be generated at the central heated region, either by means of a thermal spike[12,13] or by a non radiative exciton decay[14,15] mechanism.

On the other hand, the lifetime τ of the excited electron–hole cloud generated after every impact shows several components.[30] In fact, components at 940 μs and 1.2 ms have been derived[7] from time-resolved luminescence spectra after a nanosecond electron pulse at 2 MeV. Given the electron mobility, $\mu \approx 20\,\mathrm{cm^2\,V^{-1}\,s^{-1}}$, measured[30] at room temperature (RT) for fused quartz, as well as the transit times through the SiO_2 layer in MOS structures,[30] one can consider that the electron cloud extends over a distance L_D (i.e., the *diffusion length*) of several tens of micrometers[31] during the electron lifetime. Consequently, the size of the cloud would include a significant number of damage tracks even at the lowest fluence used in this work (10^{11} cm^{-2}).

Moreover, the light emission under irradiation results from the recombination of electron–hole pairs at certain suitable recombination centers related to the damage products.[30,32] Then, it can be deduced[33] that the luminescence yield (Y_B) of the blue band will be proportional to the irradiation flux (Φ), the energy of the incident ion (E) and the total number of available sites for exciton self-trapping [$N_B(\phi)$]; i.e., $Y_B(\phi) \propto \Phi E N_B(\phi)$. This suggests that $Y_B/\Phi E$ offers an adequate normalization for comparing the IL yields of different ions and energies, and it can be used to monitor the number of recombination (STE) centers for the blue emission generated by the irradiation, as illustrated in Fig. 2. From the initial region of this figure, one clearly sees that N_B hardly grows with fluence for irradiation with B at 3 MeV,

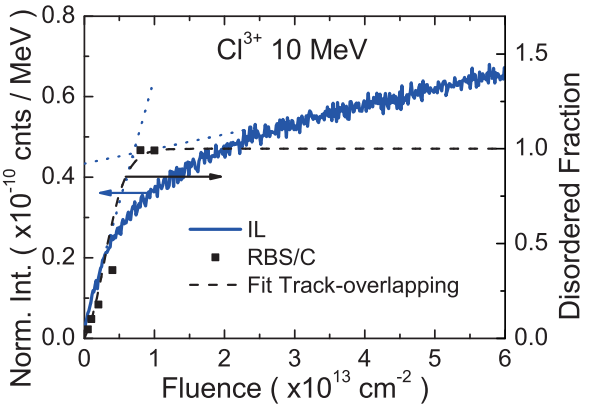

Fig. 3. Illustrative plots showing the IL (solid lines) and amorphization kinetics, measured by RBS/C (symbols) and fitted (dashed lines) by a track-overlapping model,[35] for Cl at 10 MeV. Note that the saturation fluences (crossing of the two dotted lines for the IL) nearly coincide in both cases.

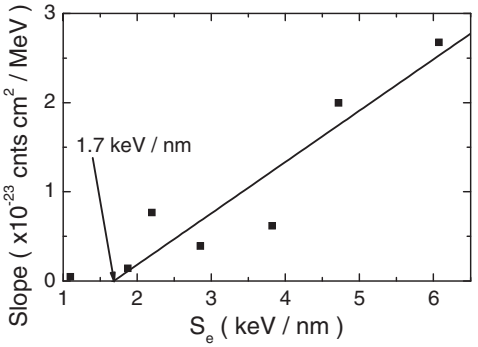

Fig. 4. Initial slope for the growth of the blue band as a function of stopping power S_e. The threshold stopping value (≈1.7 keV/nm) is determined by extrapolating the linear plot to zero yield.

whereas it increases rapidly and linearly with fluence for irradiation with Br at 25 MeV.

Now, one can go a step forward and compare the evolution of the normalized IL yield with the amorphization kinetics[24] derived from the Rutherford-backscattering spectra under channeling conditions (RBS/C). The comparison is illustrated in Fig. 3 for Cl at 10 MeV. One sees that the IL and amorphization curves are well correlated in the initial region of irradiation until the amorphization at the sample surface has been completed and the IL yield has a marked change of slope. This stage in the IL kinetics may likely have to do with the progressive increase in the thickness of the amorphized layer that has been observed in the amorphization of other dielectric crystals by swift ions.[34] In other words, the blue band constitutes a *clear signature* of heavily distorted (amorphous) regions in the irradiated quartz. Moreover, it offers a high sensitivity as one can obtain information after fluences as low as 10^{11} cm^{-2}.

Another important output of our work is the possibility of reliably determining the amorphization threshold for a single ion impact. Figure 4 shows the slope of the initial growth for the normalized yield Y_B of the blue emission band, as a function of the electronic stopping power. As we have discussed, such a slope will give the true initial growth rate for the STE band and so for the amorphized volume. One sees that the yield experiences a rapid rise with stopping power and a linear fit of the data gives a threshold value at around 1.7 keV/nm, in accordance with previous estimates obtained using a completely different method (RBS/C).[22–24]

In summary, we have shown that IL provides a unique and sensitive tool to investigate the processes of structural damage. Our data support the assignment of the 2.7 eV emission band to the recombination of self-trapped excitons and offer a reliable way to monitor the evolution of the recombination sites (strained bonds) with irradiation fluence. The threshold electronic stopping power for amorphization has been determined and is consistent with previous independent measurements. Therefore, our work opens a promising path to understand the kinetics of ion-beam amorphization and test possible models of defect formation and IL emission. Further work is in progress and will be reported elsewhere.

Acknowledgments This work has been supported by Spanish Ministry MICINN through the project MAT-2008-06794-C03-03, JCI-2009-05681, and by Madrid Community through the project TECHNOFUSION (S2009/ENE-1679). OPR is grateful to CONACyT, Mexico, for extending a postdoctoral fellowship.

1) A. Moroño and E. R. Hodgson: J. Nucl. Mater. **258–263** (1998) 1889.
2) J. F. Latkowski *et al.*: Fusion Sci. Technol. **43** (2003) 540.
3) D. L. Griscom: J. Appl. Phys. **80** (1996) 2142.
4) C. D. Marshall *et al.*: J. Non-Cryst. Solids **212** (1997) 59.
5) S. Nagata *et al.*: J. Nucl. Mater. **367–370** (2007) 1009.
6) S. I. Kononenko *et al.*: Radiat. Meas. **42** (2007) 751.
7) M. Ma *et al.*: Nucl. Instrum. Methods Phys. Res., Sect. B **268** (2010) 67.
8) L. Skuja *et al.*: Phys. Status Solidi C **2** (2005) 15.
9) K. Tanimura *et al.*: Phys. Rev. Lett. **51** (1983) 423.
10) C. Itoh *et al.*: J. Phys. C **21** (1988) 4693.
11) N. Itoh *et al.*: J. Phys.: Condens. Matter **21** (2009) 474205.
12) Z. G. Wang *et al.*: J. Phys.: Condens. Matter **6** (1994) 6733.
13) A. Kamarou *et al.*: Phys. Rev. B **73** (2006) 184107.
14) N. Itoh and M. Stoneham: *Materials Modification by Electronic Excitation* (Cambridge University Press, Cambridge, U.K., 2000).
15) A. Rivera *et al.*: Phys. Status Solidi A **206** (2009) 1109.
16) F. Agulló-López *et al.*: *Point Defects in Materials* (Academic Press, San Diego, CA, 1988).
17) R. C. Ropp: *Luminescence and the Solid State* (Elsevier, Amsterdam, 2004) 2nd ed.
18) P. D. Townsend *et al.*: *Optical Effects of Ion Implantation* (Cambridge University Press, Cambridge, U.K., 1994).
19) K. J. McCarthy *et al.*: J. Nucl. Mater. **340** (2005) 291.
20) G. E. King *et al.*: Radiat. Meas. **46** (2011) 1.
21) CMAM—Centre for Micro Analysis of Materials (2011) [http://www.cmam.uam.es/].
22) A. Meftah *et al.*: Phys. Rev. B **49** (1994) 12457.
23) S. Klaumünzer: Nucl. Instrum. Methods Phys. Res., Sect. B **225** (2004) 136.
24) J. Manzano-Santamaría *et al.*: to be published in Nucl. Instrum. Methods Phys. Res., Sect. B (2011).
25) F. Messina *et al.*: Phys. Rev. B **81** (2010) 035212.
26) A. N. Trukhin: J. Non-Cryst. Solids **149** (1992) 32.
27) R. M. Van Ginhoven *et al.*: J. Non-Cryst. Solids **352** (2006) 2589.
28) S. Ismail-Beigi and S. G. Louie: Phys. Rev. Lett. **95** (2005) 156401.
29) M. P. R. Waligórski *et al.*: Nucl. Tracks Radiat. Meas. **11** (1986) 309.
30) R. C. Hughes: Appl. Phys. Lett. **26** (1975) 436.
31) This value is probably an overestimation, because we have only considered the diffusion of electrons; holes have a much lower mobility and, presumably, the electrostatic attraction will cause the real value to be much lower, albeit, still large.
32) F. S. Goulding and Y. Stone: Science **170** (1970) 280.
33) K. Michaelian and A. Menchaca-Rocha: Phys. Rev. B **49** (1994) 15550.
34) J. Olivares *et al.*: Appl. Phys. A **81** (2005) 1465.
35) G. García *et al.*: Nucl. Instrum. Methods Phys. Res., Sect. B **269** (2011) 492.